CALIBRATING THE WATERHAMMER RESPONSE OF A FIELD PIPE NETWORK USING A MECHANICAL DAMPING MODEL

M. Stephens[1], M. Lambert[2], A. Simpson[3] and J. Vitkovsky[4]

CE Database subject headings:

Waterhammer, Water distribution systems, Model verification, Field tests

Abstract

Hydraulic transient field tests have been conducted in a water distribution network. Existing transient models are applied to model the measured responses but poor matches are obtained apart from the estimation of initial pressure rise. Possible reasons for the discrepancies include the effects of demands, entrained air, unsteady friction, friction losses associated with small lateral pipes and mechanical damping caused by the interaction of pipes and joints with surrounding soils (including the effects of vibration and different degrees of restraint). These effects are systematically investigated by inclusion of the above phenomena in conceptual transient models and calibration to the measured field responses. A mechanical damping based conceptual transient model is shown to be the only model that can be accurately calibrated to the measured field responses.

Introduction

The accurate modelling of hydraulic transient events in water supply pipe networks is becoming more important as system operators seek to understand the relationship between dynamic changes in pressure and the failure of aging pipe systems. Furthermore, the retrofit of surge mitigating infrastructure to protect existing systems, or assessment of the effect of

[1] Senior Engineer, United Water International, mstephen@civeng.adelaide.edu.au
[2] Professor, School of Civil, Environmental and Mining Engineering, the University of Adelaide, South Australia
[3] Professor, School of Civil, Environmental and Mining Engineering, the University of Adelaide, South Australia
[4] Hydrologist, Department of Environment and Resource Management, Queensland Government, Australia

new pipe interconnections, and assessment of the dynamic effects of changes in flow and pressure regimes, needs to be guided using, amongst other tools, accurate hydraulic transient models.

In this paper, the transient response of a small town water distribution network, called the Willunga Network, has been analysed. The objective is to assess the ability of existing hydraulic transient models to replicate field observations and to develop improved models. The process of developing and testing conceptual transient models, which account for a range of physical complexities, is described. A conceptual transient model that enables accurate calibration to field measurements is identified. The relatively small size of the Willunga Network enables it to be defined with accuracy. Attempts to replicate the field results with existing hydraulic transient models (typically used in commercially available software) are presented.

Background

Studies have been conducted over the last four decades to numerically simulate the effects of hydraulic transient events in water distribution networks. Kwon (2007) provides an overview of these developments and explores the use of numerical models to simulate the response of a water distribution network to hydraulic transient events. Amongst these studies, only McInnis and Karney (1995) have reported the results of field tests for a real water distribution network.

McInnis and Karney (1995) used a controlled pump trip to induce a hydraulic transient event in the Bearspaw Network in Canada. The Bearspaw Network was relatively large with a total length of approximately 90km of pipe. Most pipes in the network are concrete and there were approximately 6800 water service connections. McInnis and Karney (1995) modelled the response of the Bearspaw Network using a 1-D explicit method of characteristics solution of the governing continuity and momentum equations that describe transient flow. The model was skeletonised to remove pipes under 300mm diameter and included wave speed adjustments up to 15% to meet discretisation requirements.

McInnis and Karney (1995) developed three demand models and calibrated these to give results comparable to field measurements. However, the calibrated demand models poorly replicated the long term decay in the field measurements. Furthermore, the calibrated demands were in excess of the error estimate for the maximum system demand (and therefore unrealistic). McInnis and Karney (1995) developed an alternative quasi-steady friction factor calibration model to improve the comparison between the measured and modelled response of the Bearspaw Network without the need to calibrate demand. However, the calibration reduced the Hazen-Williams C factor from between 120-150 (for all pipes) to approximately 15. This C factor is physically infeasible for the Bearspaw Network (e.g., under steady state conditions).

Previous literature relating to the incorporation of physical complexities in network models is identified, where relevant, in various sections later in the paper.

Transient Models for Calibration to Field Responses

Parameterized transient models for the calibration of demand, such as that developed by McInnis and Karney (1995), or the calibration of entrained air, are forms of conceptual models that add complexity and may enable a model to match measured responses. The further development of parameterized transient models for demand and entrained air calibration is described by Stephens (2008). However, in the case of the Willunga Network, the direct investigations described later in this paper have eliminated these physical uncertainties. The exploration of other physical mechanisms that might contribute to the response of the Willunga Network, and the development of ways to conceptually represent such mechanisms to enable model calibration, is described below.

Fluid Friction Damping of Transients in Pipe Systems

Karney and Fillion (2003) raised the hypothesis that the flow patterns, associated with smaller lateral pipes (and potentially water service connections), may contribute to additional fluid friction losses. Even for a small network, such as the Willunga Network (which has 114 water service connections), the inclusion of each lateral pipe would require a very large model. The development of such a model is not presented in this paper.

However, detailed models, including approximated smaller lateral pipes and water service connections, for transient field tests conducted along single street water service pipes connected to the Willunga Network are presented by Stephens (2008). This work confirmed that a significant problem is the physical condition of each water service. Investigations during the field tests revealed each service could be between 5 to 80 years old and comprise galvanised iron, copper, steel, plastic or cement materials in a range of diameters and conditions. Furthermore, the extent of small diameter pipe connections to each water service could not be accurately defined within each connected private property.

A conceptual (parameterized) unsteady friction model is developed below, using a weighting function that can be calibrated to measured responses, in order to investigate the possibility that flow dependent friction losses are influencing the transient response of the Willunga Network. The model is developed for the main reticulation pipes in the Willunga Network above 100mm in diameter.

Unsteady Friction Based Conceptual Transient Model

The proposed conceptual (parameterized) unsteady friction transient model is based on a modification of the 1-D unsteady friction weighting models developed by Vardy and Brown

(1995) and Vardy and Brown (2004a) with an efficient implementation in accordance with the procedure outlined by Kagawa et al. (1983) and modified by Vitkovsky et al. (2004) for smooth and rough pipe turbulent flow. The calculation of unsteady friction involves the convolution of the change in flow with a weighting function as shown in Equation 2 (general terms in equations are defined in the notation section):

$$h_{fU} = \frac{16\nu}{gD^2 A}\left(\frac{\partial Q}{\partial t} * W\right)(t) \tag{2}$$

where W represents the unsteady friction weighting function that is convolved with flow changes throughout the transient event

Kagawa et al. (1983) defined an approximate weighting function for laminar flow, facilitating the calculation of unsteady friction within an efficient recursive calculation scheme, as shown in Equation 3:

$$W_{app}(\tau) = \sum_{k=1}^{N} m_k e^{-n_k \tau} \tag{3}$$

Values for parameters m_k and n_k are determined by fitting to the full weighting function (previously determined by Zielke (1968) for laminar flow). The value of N varies with the value of $\Delta\tau$ (the dimensionless time step equal to $4\nu\Delta t/D^2$). Kagawa et al. (1983) determined a maximum value for N of 10. The unsteady component of the total friction could then be calculated using Equation 4:

$$h_{fU}(t) = \frac{16\nu}{gD^2}\sum_{k=1}^{N} y_k(t) \tag{4}$$

In Equation 4, the recursive variable y_k at the current time step ($t+\Delta t$) is defined, in terms of the values for y_k stored for the previous time steps, the flows at the current and previous time steps and the dimensionless time step ($\Delta\tau$), using Equation 5:

$$y_k(t+\Delta t) = e^{-n_k \Delta\tau}\left(e^{-n_k \Delta\tau} y_k(t) + m_k\left[V(t+\Delta t) - V(t)\right]\right) \quad (5)$$

Vitkovsky et al. (2004) directly adapted the efficient recursive approximation developed by Kagawa et al. (1983) for rough pipe turbulent flow conditions using scaling coefficients for parameters m_k and n_k based on the initial flow condition and/or roughness in each pipe in a network.

The efficient recursive approximation used to represent the weighting function for the calculation of unsteady friction (without any parameterisation) utilises N = 10 values of parameters $m_{k=1,10}$ and $n_{k=1,10}$ (refer to Kagawa et al. (1983) or Vitkovsky et al. (2004)). Two additional parameters, named $m_{k=11}$ and $n_{k=11}$, are introduced in this paper to parameterise the representation of the weighting function and thereby create a conceptual model with $N+1$ = 11 values defined the conceptualised weighting function.

Values for $m_{k=1,10}$ and $n_{k=1,10}$ are pre-determined and are not calibrated (i.e., the values required to approximate the theoretical weighting function for rough pipe turbulent flow determined by Vitkovsky et al. (2004) are applied without alteration). However, the values for the conceptual parameters $m_{k=11}$ and $n_{k=11}$ are not pre-determined (i.e., have no pre-determined theoretical value and need to be calibrated using measured transient responses). This parameterized model allows for values of $m_{k=11}$ and $n_{k=11}$ to be calibrated to achieve the best least squares fit between measured and predicted transient responses (any non-zero values for the two conceptual parameters will artificially modify the shape of the theoretical weighting function which becomes a parameterized weighting function). The parameterized model facilitates calibration for flow dependent friction losses influencing the transient response of the Willunga Network without requiring the pre-determination of the diameter and condition of all lateral pipes in the network.

Mechanical Damping of Transients in Pipe Systems

Williams (1977) confirmed that pipes with flexible joints, which are not completely restrained, will absorb a significant proportion of the energy of any internal fluid transient. Budny et al. (1991) subsequently performed a series of laboratory experiments on a 47.7m long copper pipeline system investigating the impact of restraint conditions on transient damping. Budny et al. (1991) calibrated a viscous damping coefficient to approximate experimentally measured damping caused by mechanical motion and vibration for different restraints applied to their laboratory apparatus. Non-viscous forms of damping, including inertial, structural or Coulomb damping, were all represented using equivalent viscous damping.

Flexible joints typically occur at 3m to 10m intervals along buried metal and cement pipelines, depending on the diameter of the pipeline, and are used for small distribution as well as large transmission pipelines (the AC pipe comprising the Willunga Network is flexibly jointed). Elastomeric gaskets or rubber rings are typically used to seal the joints while permitting axial movement and rotation up to approximately 3 to 4 degrees. Each flexible joint, at which longitudinal and lateral movement is possible through circumferential expansion and longitudinal sliding, has the potential to introduce damping.

For buried pipelines, the presence of continuous soil strata in contact with the pipe walls provides a direct external viscous damping mechanism for dissipating internal transient energy. The amount of energy dissipated will be correlated with the stiffness of the pipe wall (i.e., pipe wall material and condition). Furthermore, the soil is an important factor when assessing the restraint of the pipeline. Buried field pipelines are restrained by surrounding soils and thrust blocks. Soil strata provide variable support to buried pipelines such that the degree of restraint, and potential motion and vibration, are a function of variations in soil strength and compaction (degree of contact).

Equivalent Viscous Damping Mechanism

It is difficult to model the effect of restraints, flexible joints and soil/pipe interaction upon the damping of the measured transient response of a pipeline. In the context of their laboratory experiments on water pipelines, Williams (1977) and Budny et al. (1991) noted that, in the absence of a more detailed understanding of the physics of the damping mechanisms affecting a pipeline, and the practical level of physical information required to model all of the potential energy losses, viscous damping mechanisms and coefficients could be introduced to a transient model to incorporate equivalent dispersion and damping. A conceptual (parameterized) transient model, incorporating mechanical dispersion and damping, has been developed by including a single-element Kelvin-Voigt viscoelastic mechanism. This mechanism is used to replicate mechanical dispersion and damping using creep deformation spring and dashpot retardation time parameters calibrated to measured responses.

Kelvin-Voigt Mechanical Model

Viscoelastic models for the stress/strain relationship in the walls of plastic pipelines, under transient and other pressure conditions, have developed since the introduction of such pipelines in the mid-1970s. Gally et al. (1979) extended the basic equations for fluid transients to include a time dependent creep compliance function as described below.

The effect of a viscoelastic pipe wall response is incorporated by the inclusion of a third term, incorporating a retarded strain effect in the pipe wall, in the governing water hammer continuity equation as shown in Equation 6:

$$\frac{\partial H}{\partial t} + \frac{a^2}{gA}\frac{\partial Q}{\partial x} + \frac{2a^2}{g}\frac{\partial \varepsilon_r}{\partial t} = 0 \qquad (6)$$

where ε_r = the circumferential strain in the pipe wall

A single-element Kelvin-Voigt viscoelastic mechanism, comprising a spring and dashpot element as shown in Figure 1, can be applied to determine the creep compliance function used in the calculation of the retarded strain term in the modified continuity equation.

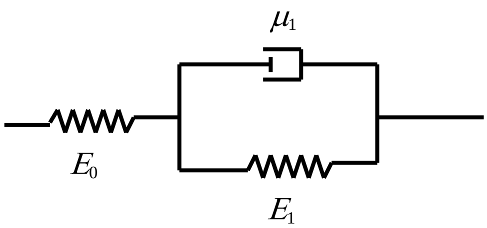

Figure 1 – Single-element Kelvin-Voigt viscoelastic mechanism

In Figure 1, E_0 is the elastic modulus of the pipe wall, with J_0=1/E_0, the compliance of the elastic spring, and E_1 the modulus of elasticity of the creep deformation spring. The viscosity of the dashpot μ_1 represents the viscous creep behaviour. Further parameters J_1 and τ_1 are defined as J_1=1/E_1, the compliance of the creep deformation spring, and τ_1= μ_1/E_1, the retardation time of the dashpot. These later two components appear in an expression describing the creep compliance function for the pipe wall as shown in Equation 7:

$$J(t) = J_0 + J_1(1 - e^{-t/\tau_1}) \tag{7}$$

The evaluation of the rate of change of strain in a pipe wall, as required for the calculation of the third term in Equation 6, can now be performed using Equation 8 and Equation 9 originally presented by Gally et al. (1979):

$$\varepsilon_r(x,t) = \frac{\alpha D}{2h}\gamma\int_0^t \left[H(x,t-t') - H_0(x)\right]\frac{J_1}{\tau_1}e^{\frac{-t'}{\tau_1}}dt' \tag{8}$$

$$\frac{\partial \varepsilon_r(x,t)}{\partial t} = \frac{\alpha D}{2h}\frac{J_1}{\tau_1}\gamma\left[H(x,t) - H_0(x)\right] - \frac{\varepsilon_r(x,t)}{\tau_1} \tag{9}$$

In Equation 9, $\varepsilon_r(x,t)$ = the strain in the pipe wall, $\partial\varepsilon_r(x,t)/\partial t$ = the rate of change of strain in the pipe wall, h = pipe wall thickness and α = wall thickness factor

Efficient Solver for Viscoelastic Calculations

An efficient solver is required to facilitate the inverse calibration of the mechanical damping based conceptual transient model presented below. The calculation of the integral in Equation 8 involves a convolution of the change in pressure head (relative to the steady state pressure head $H_0(x)$) with the function describing the non-elastic creep of the pipe wall (i.e., a creep compliance function). Equation 8 can be expressed in the form shown in Equation 10:

$$\varepsilon_r(x,t) = \frac{\alpha D}{2h}\gamma\left(\frac{\partial H}{\partial t} * J\right)(t) \tag{10}$$

where J represents the creep compliance function that is convolved with pressure head changes throughout the transient event

Equation 10 is analogous to the equation developed by Vitkovsky et al. (2004), used in the efficient calculation of unsteady friction with a one-dimensional weighting function, and both equations involve the calculation of a convolution integral. As a consequence, the recursive approximation developed by Kagawa et al. (1983) for the efficient calculation of unsteady friction can be applied to the calculation of the strain in the wall of a pipe exhibiting viscoelastic behavior using Equation 11:

$$\varepsilon_r(x,t) = \frac{\alpha D}{2h}\gamma\sum_{m=1}^{N} y_m(t) \tag{11}$$

in which N = the number of elements in the mechanical model and the variables y_m are defined using Equation 12:

$$y_m(t+\Delta t) = e^{-\Delta t/\tau_m} y_m(t) + \frac{J_m}{\tau_m} e^{-\Delta t/\tau_m}\left[H(t+\Delta t) - H(t)\right] \tag{12}$$

which reduces to Equation 13:

$$y_1(t+\Delta t) = e^{-\Delta t/\tau_1} y_1(t) + \frac{J_1}{\tau_1} e^{-\Delta t/\tau_1}\left[H(t+\Delta t) - H(t)\right] \tag{13}$$

for a model with a single-element Kelvin-Voigt visocelastic mechanism and a creep compliance function defined by Equation 14:

$$J(t) = J_1\left(1 - e^{-t/\tau_1}\right) \tag{14}$$

In Equation 14, J_1 is the compliance of the creep deformation spring, τ_1 is the retardation time of the dashpot, y_1 is the recursive variable and *J(t)* is the creep compliance function for a single-element Kelvin-Voigt model. The elastic component of the wall deformation (i.e., J_0) is removed so that only the viscous component of the viscoelastic behaviour is replicated (in the context of transient analysis, the elastic component of the pipe response is determined in the normal system of equations and is proportional to the wave speed).

Mechanical Damping Based Conceptual Transient Model

The Asbestos Cement (AC) pipes comprising the Willunga Network are not viscoelastic (this was validated by Stephens (2008) who conducted load versus deformation tests on a section of AC pipe from the Willunga Network confirming linear elastic behaviour). Therefore, the initial values for the creep deformation spring and dashpot retardation time parameters are zero (i.e., the AC pipe behaves in a linear elastic fashion). However, non-zero values modify the shape of the creep compliance curve used in the calculation of viscous dispersion and damping. The Kelvin-Voigt element is applied uniformly at each computational node in the network model, in addition to algorithms for the effects of known demand/leakage, quasi-steady friction and unsteady friction, to complete the model of the Willunga Network. Parameters J_1 and τ_1 are calibrated to achieve the best least squares fit between measured and predicted responses. The subscript 1 is applied because there is only one creep deformation spring and one dashpot retardation time parameter.

Use of Error Variance to Assess Calibration Results

The ability of conceptual transient models that are developed to replicate measured responses will be quantified using the error variance (s^2) for the data points comprising measured and modelled response vectors (i.e., pressure versus time). The error variance is proportional to the sum of the square of the differences between the measured and modelled responses (i.e., proportional to the objective function) and represents the unbiased sample variance of the model error after calibration (i.e., the objective function divided by the number of data points minus the number of model parameters) as shown in Equation 1:

$$s^2 = \frac{1}{M - N} \sum_{i=1}^{M} \left(H_i^m - H_i \right)^2 \qquad (1)$$

where M is the number of measured data points, N is the number of model parameters, H_i^m is the measured pressure response and H_i is the predicted pressure response

Field Tests on the Willunga Network

Composition and Operation of Willunga Network

The Willunga Network, as shown in Figure 2, is located in South Australia and comprises approximately 4km of 100mm to 150mm nominal diameter Asbestos Cement (AC) pipe. The boundaries to the Willunga Network comprise the Willunga storage (a 2.2 ML concrete tank) and a ring of closed valves separating the Willunga network from the remainder of the larger network system. The majority of these isolation valves are permanently closed to delineate a boundary between the extent of system supplied by the Willunga tank and a pumped transmission main from an adjacent township. A pump station refills the Willunga tank every 1 to 4 days depending on changes in demand from summer to winter. SCADA telemetry is available and can be accessed to undertake real-time monitoring of the water levels in the Willunga tank.

Setup and Conduct of Controlled Transient Field Tests

Figure 2 shows the general configuration of the Willunga Network during the transient field tests (as well as the topological setup for the transient models). Transient field tests were undertaken with the transient generator installed at two separate locations shown as points A and B. Pressure measurement stations 1, 2 and 3 were deployed for the tests with the transient generator installed at point A. Only stations 2 and 3 were deployed for the tests with the transient generator installed at point B (station 1 was re-deployed to measure the pressure response within the top section of the transient generator for these tests). Each pressure measurement station included a Druck PDCR-810 pressure transducer mounted in a "dummy" fire plug and all measurement stations were synchronised using a cable system. The recording rate for the pressure transducers was 500Hz for all tests.

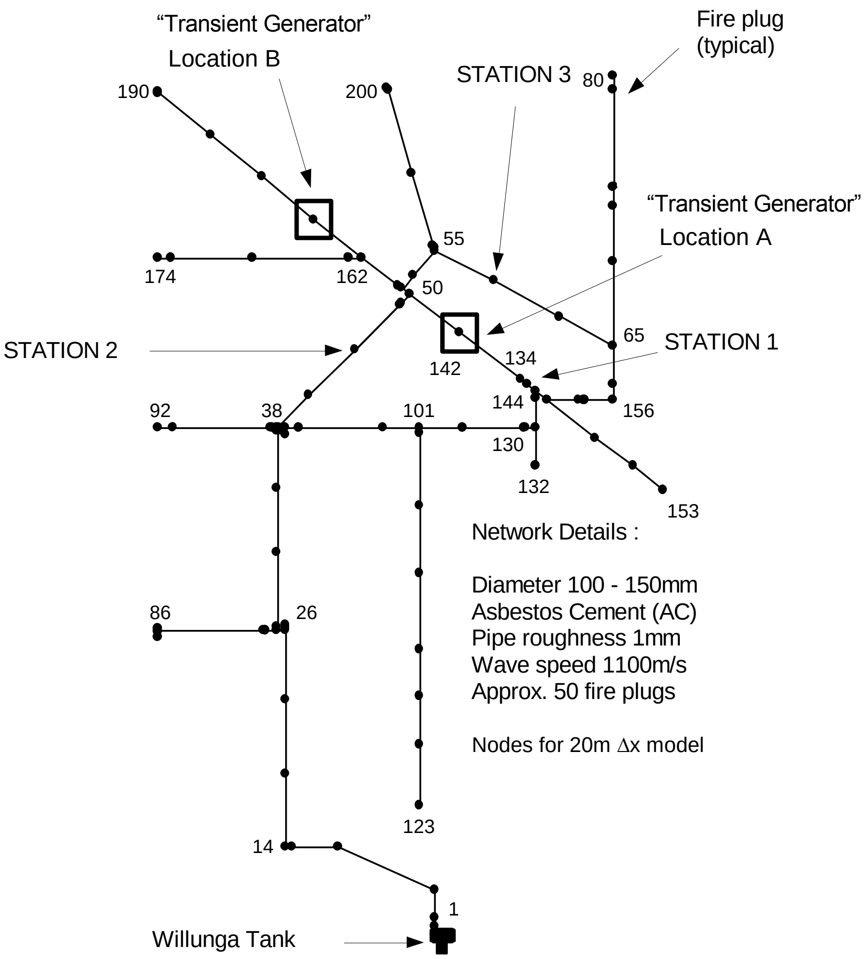

Figure 2 – Schematic of Willunga Network showing transient test locations, fire plug and isolation valve locations and the topological setup for transient modelling

Controlled transients were induced by a transient generator comprising a small ball valve (15 mm diameter) that was closed rapidly. The ball valve is located immediately upstream of a discharge nozzle (15mm diameter when the transient generator was located at point A), on the end of a 1.25m high standpipe (which is, in turn, mounted on existing fire plugs). A torsion spring, mounted near the end of the standpipe and coupled to the 15 mm ball valve, was used to mechanically close the flow regulating ball valve in approximately 4ms. A 10mm discharge nozzle was installed when the transient generator was located at point B. Figure 3 shows the typical installation of the transient generator during the field tests on the Willunga Network.

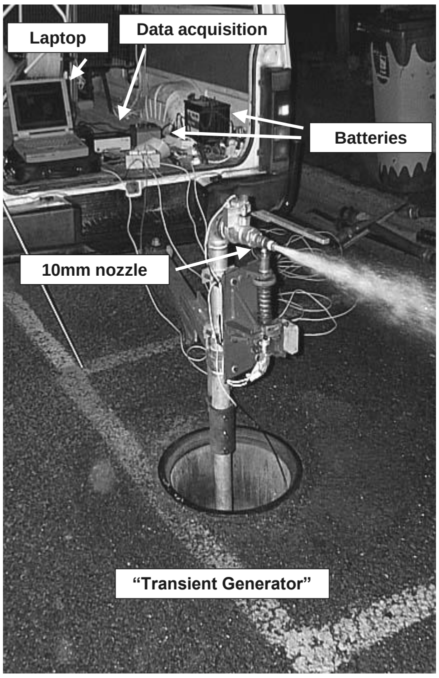

Figure 3 – Mechanical elements comprising the Transient Generator with data acquisition instrumentation used in field tests on the Willunga Network

Figure 4 shows the typical installation of a pressure measurement transducer on an existing fire plug within the Willunga Network (specifically, at station 1 shown in Figure 2). The pressure transducers were mounted inside “dummy” plug connectors that are normally used to blank-off a fire plug/air valve or fire plug discharge outlet. The “dummy” plugs were cored-out to create a void in which the pressure transducer could be accommodated and sealed.

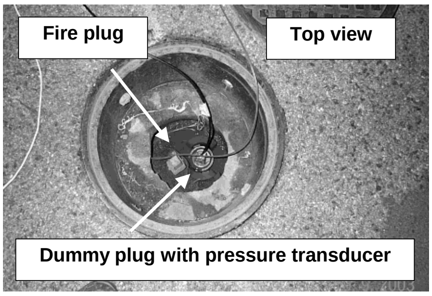

Figure 4 – Top view of the installation of a pressure transducer in a fire plug at measurement station 1 in the Willunga Network

Background Demand and Leakage

To reduce the impact of demand, the transient tests were conducted during the night from approximately 12:00 midnight to 5:00 am. Notices were issued to customers to not use water during this period and this had the effect of minimising demand. Remaining demand and leakage were directly measured using the available SCADA telemetry for the tank supplying the Willunga Network between 12:00 midnight and 5:00 am. Both the SCADA telemetry and digital display for tank level were checked at 12.00 midnight and 5.00 am to confirm the quantity of water that had been drawn from the tank during the period of testing.

The volume drawn from the tank during the test period comprised water used in the tests (i.e., discharged through the transient generator) and background demand and leakage. Steady state modelling of the Willunga Network was used to determine the flow through the transient generator and enabled the average unaccounted for demand and leakage to be determined. For details of this modelling refer to Stephens (2008). An average distributed background demand and leakage of 0.68 L/s was calculated for the entire Willunga Network during the test period (i.e., the average total demand and leakage attributable to customers supplied by the network was, on average, 0.68 L/s over the 5 hr test period).

Assessment of Air Content

The Willunga Network includes approximately 50 fire plugs that each comprise a pipe riser connecting the main pipe to a hydrant valve in a chamber just below the road surface level. To reduce the possibility of any significant discrete air pockets being present, all the fire plugs were flushed within the Willunga Network approximately six hours prior to the test period. No significant quantity of air was released during the flushing.

Development of Transient Models of the Willunga Network

Quasi-Steady and Unsteady Friction Transient Model

A 1-D method of characteristics (MOC) solution of the governing continuity and momentum equations that describe transient flow has been developed for pipe networks employing cubic polynomial spaceline interpolation in an implicit solution scheme. The model is similar to that employed by McInnis and Karney (1995) except that the system of equations describing state variables Q (flow) or V (velocity) and H (pressure head), together with boundary conditions, are solved simultaneously at all network junctions rather than junction by junction for each time step.

The model provides for the calculation of the effects of quasi-steady and unsteady friction (primarily using efficient recursive approximations for unsteady friction weighting functions for laminar, smooth pipe turbulent and rough pipe turbulent flow regimes – see Vitkovsky et al. (2004)), discrete air pockets and entrained air (using the discrete gas cavity model developed by Wylie (1984) and adapted for an implicit implementation), viscoelasticity (for the analysis of plastic pipes) and quasi-steady minor losses.

Wave Speed

The wave speed for the AC pipe comprising the Willunga Network has an average value of 1100 m/s (with a minimum of 1040 m/s and maximum of 1150 m/s) for 12 field tests conducted at locations A and B. This average wave speed applies for the pipeline paths between the measurement stations shown in Figure 2. The wave speeds were determined using the arrival times of measured pressure wavefronts and the potentiometer record for the closure of the ball valve mounted in the transient generator during each test. The potentiometer was mounted on the shaft of the ball and its voltage output varied as the ball valve rotated during closure. Typical wavefronts, and a potentiometer record, are shown in

Figure 5. The wavefronts were sharp, because the torsion spring closed the ball valve in a very short time (approximately 4 ms), and this enabled the wave speeds to be accurately determined.

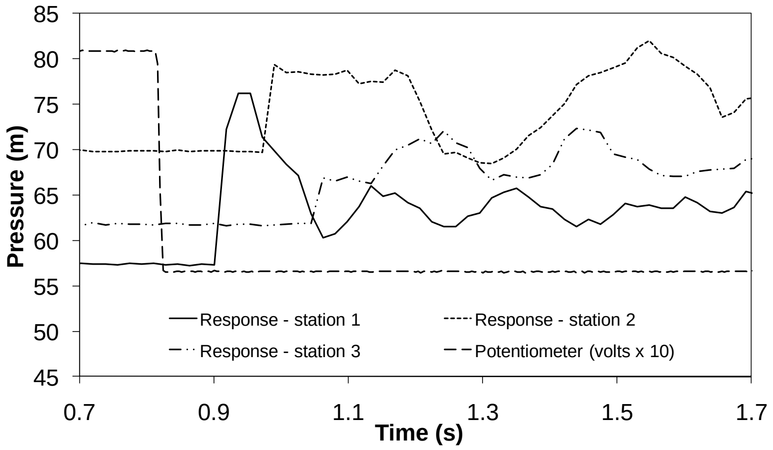

Figure 5 – Measured transient wavefronts at measurement stations 1, 2 and 3 in the Willunga Network with the potentiometer record for the ball valve in the Transient Generator

Topological Setup for Numerical Model

A transient model has been developed for the Willunga Network, as shown in Figure 2, with a 20 m pipe reach discretisation. This discretisation gives rise to 201 pipe reaches and 200 nodes (excluding an additional 6 nodes used to represent valves). Figure 2 shows node numbers at major junctions and fire hydrant locations.

In order to maintain a Courant number of 1.0 a 1.9 % average adjustment to the true pipe lengths was required to avoid the need to use an interpolation scheme. The sensitivity of the results to model discretisation was assessed by developing another transient model with a 10m pipe reach discretisation. For this model, a 1.4 % average adjustment to the true pipe lengths was required to avoid interpolation. The results obtained with the two different discretisations are similar, as shown in Figure 6 for predicted responses at station 2, and confirm that the 20 m pipe reach discretisation is sufficient.

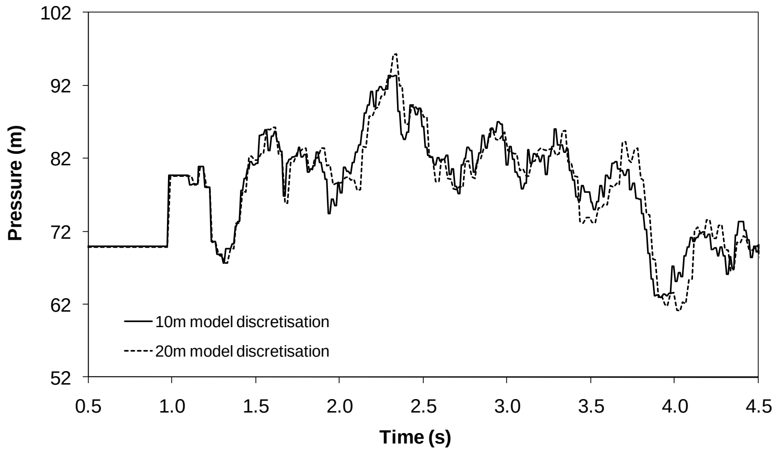

Figure 6 – Comparison of predicted transient model responses at station 2 in the Willunga Network with 10m and 20m discretisations

Average Pipe Roughness

CCTV camera footage of approximately 70 m of pipeline was available from two branches within the Willunga Network. This footage revealed that the interior of the AC pipe was in relatively good condition. Roughness height values of the order of 1 mm were qualitatively gauged from the CCTV camera footage with occasional nodules and other build up at joints. Table 1 relates the nodes shown in Figure 2 to specific pipeline diameters, network flows during the tests with the transient generator at point A and the corresponding Reynolds number variations throughout the network. The Reynolds Numbers for flow throughout the network range from 338 to 35213 and are low. Due to the low flow and Reynolds Numbers, the predicted steady state pressures at the three measurement stations are insensitive to small variations in pipeline roughness. The qualitatively gauged roughness height of 1mm was adopted for the transient modelling.

Table 1 – Pipe numbers, nodes, diameters, network flows and Reynolds Numbers

Pipe Number	Pipe Nodes	Pipe Length (m)	Pipe Diameter (m)	Flow (L/s)	Reynolds No.
1	1-14	257.4	0.231	4.61	22289
2	14-26	237.6	0.231	4.61	22289
3	26-38	237.6	0.144	4.54	35213
4	38-50	237.6	0.096	2.46	28620
5	50-55	99.0	0.096	0.11	1280
6	55-65	198.0	0.096	0.18	2094
7	65-80	297.0	0.096	0.07	814
8	26-86	118.8	0.231	0.07	338
9	38-92	118.8	0.096	0.08	931
10	38-101	178.2	0.096	2.01	23385
11	101-123	435.6	0.096	0.04	465
12	101-130	138.6	0.096	1.96	22803
12a	130-132	39.6	0.096	0.06	698
13	130-144	39.6	0.096	1.91	22221
13a	134-144	39.6	0.096	1.60	18615
14	144-153	178.2	0.096	0.05	582
15	65-144	118.8	0.096	0.26	3025
16	50-142	79.2	0.144	2.42	18770
16a	134-142	118.8	0.144	1.60	12410
17	50-162	79.2	0.144	0.15	1163
18	162-174	237.6	0.096	0.08	931
19	162-190	316.8	0.144	0.08	621
20	55-200	198.0	0.096	0.07	814

Minor Losses

While the influence of minor losses was not expected to be significant for the Willunga Network (given the relatively long pipe lengths and the presence of only five bends and ten junctions), a quasi-steady minor loss approximation has nevertheless been implemented. The additional minor loss was incorporated using equivalent pipe lengths and wall friction to represent minor losses at model nodes. The lack of sensitivity of the predicted response of the Willunga Network to the inclusion and omission of minor losses is illustrated in Figure 7 (at station 2 for a typical test conducted with the transient generator located at point A). The quasi-steady minor losses do not have any significant impact on the predicted transient response of the Willunga Network for a typical test flow of up to 5L/s to the transient generator.

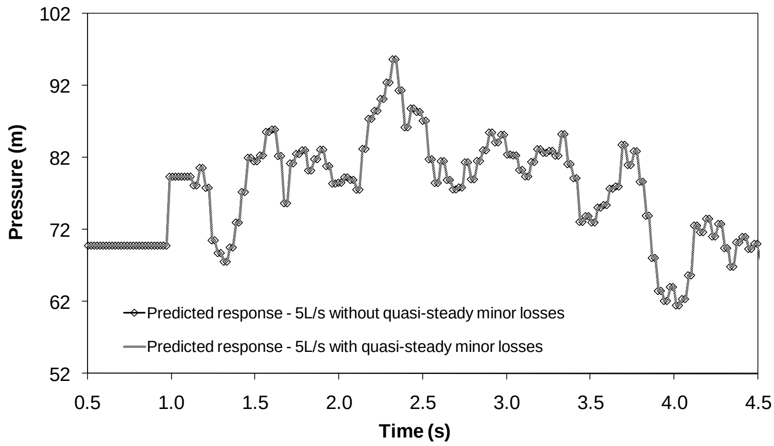

Figure 7 – Numerical modelling of predicted response of Willunga Network at station 2 using a quasi-steady friction transient model with and without minor losses

Comparison of Field Tests with Transient Model Results

The comparison between the measured and modelled transient responses of the Willunga Network at station 2, for a typical controlled transient test over a time scale of 4s, is illustrated in Figure 8. In addition, the comparison over a longer time scale of 14s is illustrated in Figure 9. The results shown are indicative of the results obtained at the other two measurement locations. The average distributed background demand and leakage of 0.68L/s was included by equal distribution at 10 boundary nodes. Based on the investigation described above, discrete air pockets and entrained air were not included in the model.

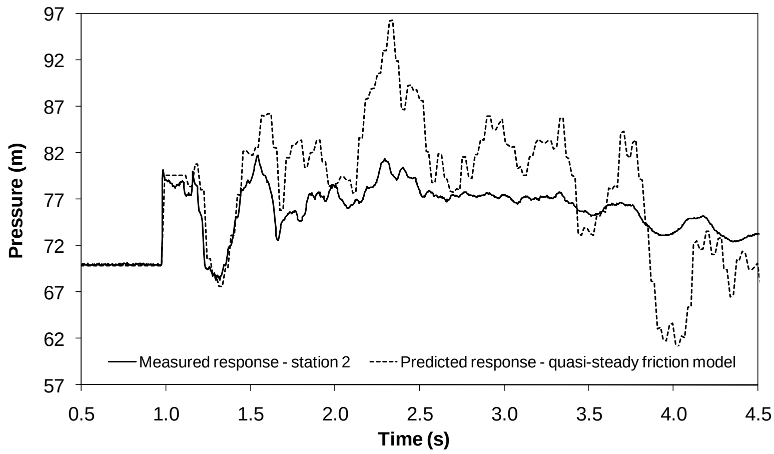

Figure 8 – Measured and predicted responses for station 2 in the Willunga Network using a quasi-steady friction transient model over 4s

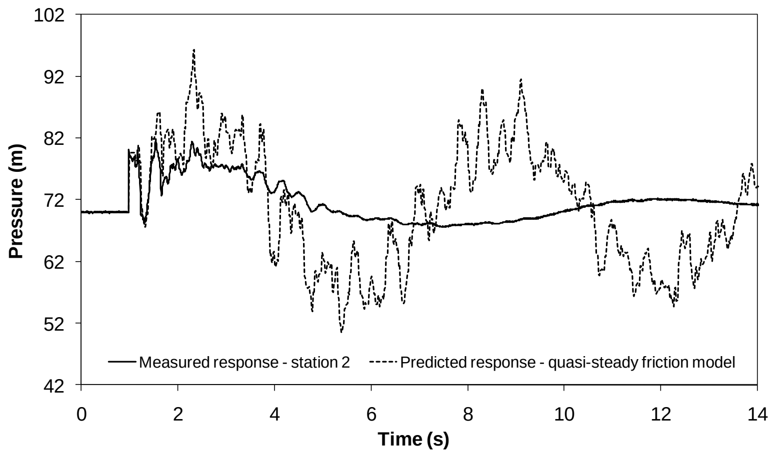

Figure 9 – Measured and predicted responses for station 2 in the Willunga Network using a quasi-steady friction transient model over 14s

The transient model with quasi-steady friction (no unsteady friction) and minor loss approximations described above adequately predicts the magnitude and form of the initial surge. However, the predicted response, obtained using the traditional transient model, exhibits insufficient dispersion and damping after the initial surge and becomes progressively further out of phase. The error variance for the fit between the measured and modelled transient responses of the Willunga Network at measurement stations 1, 2 and 3 (i.e., using the measured and predicted responses at all measurement stations) is 265.7.

Contribution of unsteady friction to Willunga Network response

The theoretical effect of unsteady friction was implemented using the rough pipe turbulent weighting function and efficient recursive approximation, developed by Vitkovsky et al. (2004), as adapted for a network transient model of the Willunga Network with a 20 m discretisation. The rough pipe turbulent weighting function has been used because the average pipe roughness was approximately 1 mm and a mix of turbulent and laminar flow conditions were established along different pipes within the Willunga Network during the tests.

Figure 10 shows, at station 2, that the theoretical contribution of unsteady friction along the main pipes is not significant for the flow conditions that existed during tests on the Willunga Network (as listed in Table 1 above) for the tests conducted with the transient generator located at point A. The error variance for the fit between the measured and modelled transient responses of the Willunga Network at all three measurement stations, obtained using a transient model including the theoretical contribution of unsteady friction, is 261.0 (compared with 265.7 for the fit obtained using the transient model with quasi-steady friction only). There is only a marginal improvement in model accuracy when the theoretical contribution of unsteady friction is taken into account.

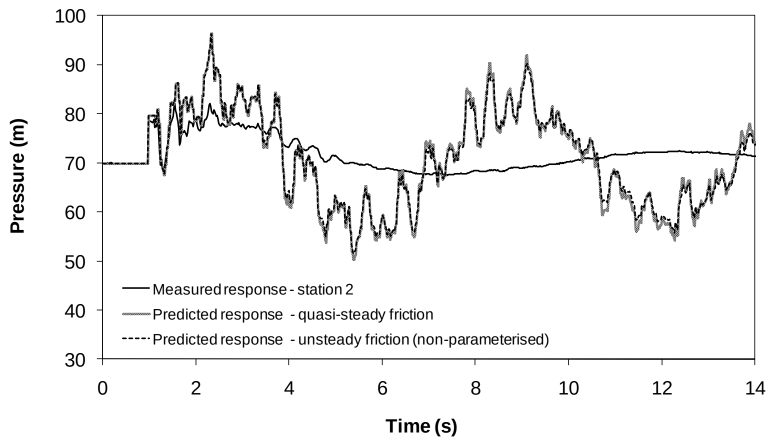

Figure 10 – Measured and predicted responses for station 2 showing insignificant additional friction loss due to unsteady friction (non-parameterized)

Calibration of Conceptual Transient Models to Measured Responses

Calibration of Unsteady Friction Based Conceptual Transient Model

Table 2 summarises the parameter estimates (i.e., the fitted values for $m_{k=11}$ and $n_{k=11}$), the parameter standard deviations and the error variances obtained when the conceptual unsteady friction model is calibrated to the measured responses for a typical field test on the Willunga Network. Inverse analysis has been performed using 20m, 40m and 80m pipe reach discretisations, without interpolation, to assess the sensitivity of the global calibration mechanism to model discretisation. Inverse analysis was performed using a 14s long record of the measured pressure responses at stations 1, 2 and 3 (i.e., all available measured and predicted responses are used in the determination of the error variance). The known demand and leakage (a total of 0.68L/s demand and leakage over the duration of the test period) was included in the model.

Table 2 – Parameter estimates and error variances for conceptual unsteady friction model after calibration to measured responses at stations 1, 2 and 3

Model (Δx)	Mean Value from Fitting		Std Deviation		Error Variance (m^2)
	$m_{k=11}$	$n_{k=11}$	$m_{k=11}$	$n_{k=11}$	
20m	1454	4297	6.6	34.8	55.3
40m	1429	4299	9.0	48.6	61.7
80m	1420	4235	12.5	68.0	57.3
Average	1434	4277	NA	NA	58.1

Both the fitted parameter values and error variances were consistent for each model discretisation. Furthermore, the standard deviations for the parameters $m_{k=11}$ and $n_{k=11}$ are less than the fitted values by an order of magnitude in all cases. This confirms that the response of the model is sensitive to the fitted values of $m_{k=11}$ and $n_{k=11}$ and that the parameterized unsteady friction model does not have redundant parameters.

The error variance when both $m_{k=11}$ and $n_{k=11}$ are equal to zero is 261.0 (i.e., the error variance obtained using a transient model when the theoretical contribution of unsteady friction (non-parameterized) is taken into account). The application of the conceptual unsteady friction model has therefore significantly improved the fit between measured and predicted responses without the need to calibrate demand or a percentage of entrained air that is physically inconsistent with observations.

Figure 11 shows the effect of parameters $m_{k=11}$ and $n_{k=11}$ on the weighting function used in the calculation of calibrated unsteady friction and a comparison with the unmodified weighting function. The calibration does not influence the non-parameterized weighting function for dimensionless times greater than approximately 0.001. This threshold corresponds to a time approximately 2.2s after the beginning of the analysis and between 1.15s and 1.30s after the controlled transient is induced in the Willunga Network. These times correspond to the point at which a significant discrepancy between the measured and predicted responses is observed.

The modified weighting function is conceptual and is being used to calibrate for dispersion and damping effects (from the postulated flow effects associated with smaller lateral pipes) that are not directly related to the theoretical affect of unsteady friction along the main reticulation pipes.

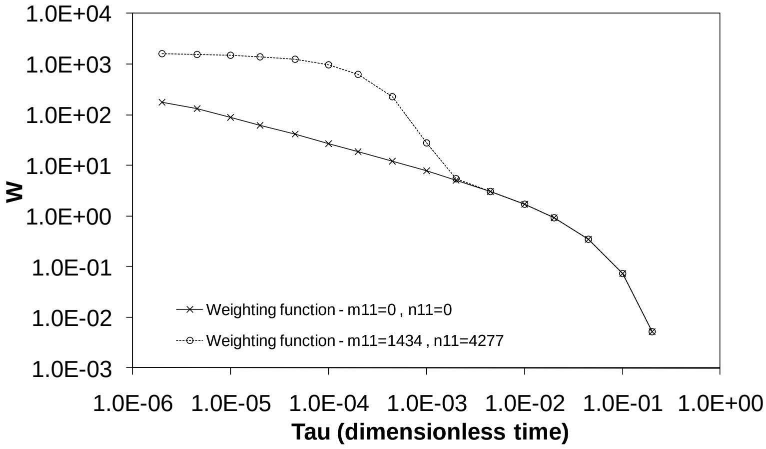

Figure 11 – Theoretical (non-parameterized) and parameterized unsteady friction weighting functions after calibration of the conceptual unsteady friction transient model

The comparison between the measured and calibrated transient responses of the Willunga Network at station 2, for a typical controlled transient test over a time scale of 4s, is illustrated in Figure 12. The comparison over a time scale of 14s is illustrated in Figure 13. The calibrated transient response was obtained using the model with a 20m pipe reach discretisation.

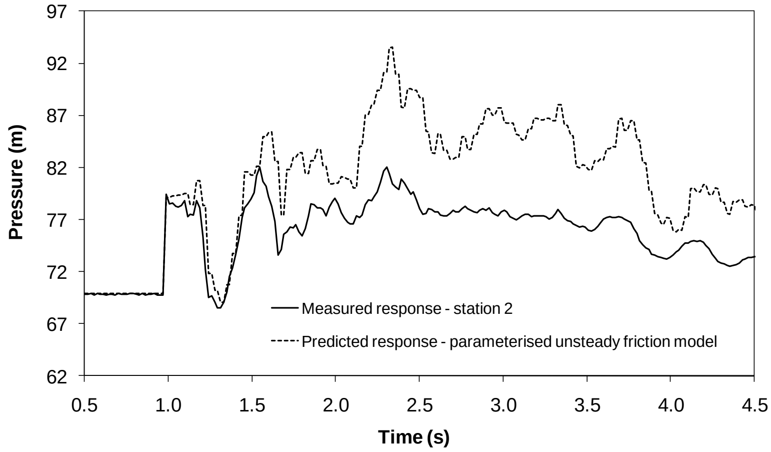

Figure 12 – Measured and predicted responses for station 2 in the Willunga Network using a conceptual (parameterized) unsteady friction model over a time period of 4s

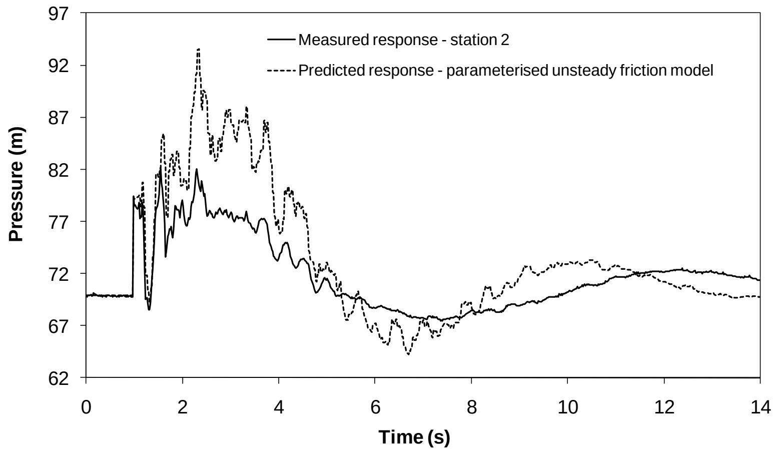

Figure 13 – Measured and predicted responses for station 2 in the Willunga Network using a conceptual (parameterized) unsteady friction model over a time period of 14s

Because the unsteady friction mechanism introduces dispersion with damping, a balance has been struck between the two during the inverse calibration. The prediction of long term dispersion and damping is improved, relative to the results for the quasi-steady and unsteady (non-parameterized) friction transient models presented above, as shown in Figure 13. However, the comparison deteriorates over the time scale of the initial surge as shown in Figure 12.

Calibration of Mechanical Damping Based Conceptual Transient Model

Table 3 summarises the parameter estimates (i.e., the fitted values for the creep deformation spring (J_1) and dashpot retardation time (τ_1)), the parameter standard deviations and the error variances obtained when the viscous dispersion and damping model is calibrated to the measured responses for a typical field test. Inverse analysis has been performed using 20m, 40m and 80m pipe reach discretisations, without interpolation, to assess the sensitivity of the results to model discretisation. Inverse analysis was performed using a 14s long record of the measured pressure responses at stations 1, 2 and 3 (i.e., all available measured and predicted responses are used in the determination of the error variance). The known demand and leakage (a total of 0.68L/s demand and leakage over the duration of the test period) was included in the model. Furthermore, the theoretical, not calibrated, contribution of unsteady friction was included in the model.

Table 3 – Parameter estimates and error variances for conceptual mechanical damping model after calibration to measured responses at stations 1, 2 and 3

Model (Δx)	Mean Value from Fitting		Std Deviation		Error Variance (m^2)
	J_1x10^{-10} (Pa^{-1})	τ_1 (s)	J_1x10^{-12} (Pa^{-1})	τ_1x10^{-1} (s)	
20m	0.290	1.528	0.253	0.185	1.92
40m	0.301	1.577	0.370	0.268	4.59
80m	0.306	1.648	0.540	0.399	3.33
Average	0.299	1.584	NA	NA	3.28

Both the fitted parameter values and error variances were consistent for the three model discretisations. Furthermore, the standard deviations for the parameters J_1 and τ_1, as shown in Table 3, are less than the fitted values of parameters J_1 and τ_1 by an order of magnitude in all cases. This confirms that the response of the model is sensitive to the fitted values of J_1 and τ_1 and that the parameterized mechanical damping model does not have redundant parameters.

Figure 14 shows the calibrated creep compliance function and a comparison with a creep compliance function for a polyethylene pipe tested by Covas et al. (2004). The calibrated creep compliance function is an order of magnitude smaller for the Willunga Network than that which Covas et al. (2004) determined for a laboratory polyethylene pipe. The calibration of a creep compliance function for the Willunga Network is conceptual or artificial because it is being used to compensate for viscous dispersion and damping that is related to mechanical damping. This mechanical damping derives from the effects of mechanical motion and vibration, flexible joints and soil/pipe (joint) interaction.

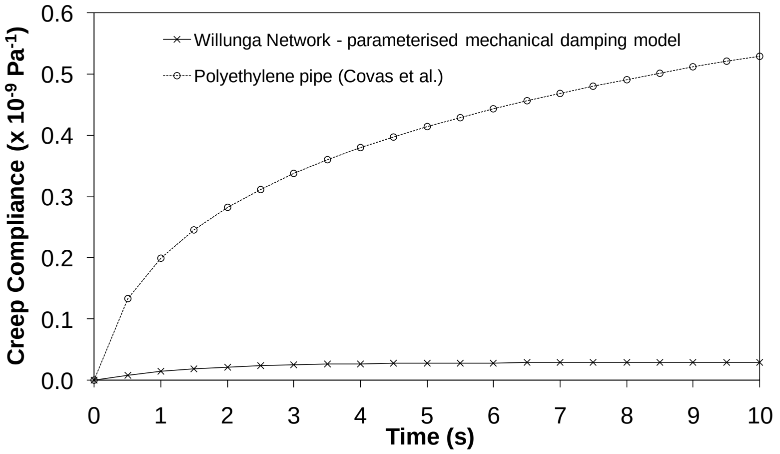

Figure 14 – Comparison of the parameterized creep compliance function for the Willunga Network, after calibration of the conceptual mechanical damping transient model, with the creep compliance function for a polyethylene laboratory network

Figure 15 shows the calibrated creep compliance function at a magnified scale. As for the parameterized unsteady friction weighting function, the shape of the creep compliance function allows for global dispersion and damping to be introduced. The effect of the calibrated viscous damping is immediate but continues to increase such that at a time equal to 2 seconds the creep compliance function has reached 73 % of its maximum value of 0.0285 x 10^{-9} Pa^{-1} (reached at time 10s).

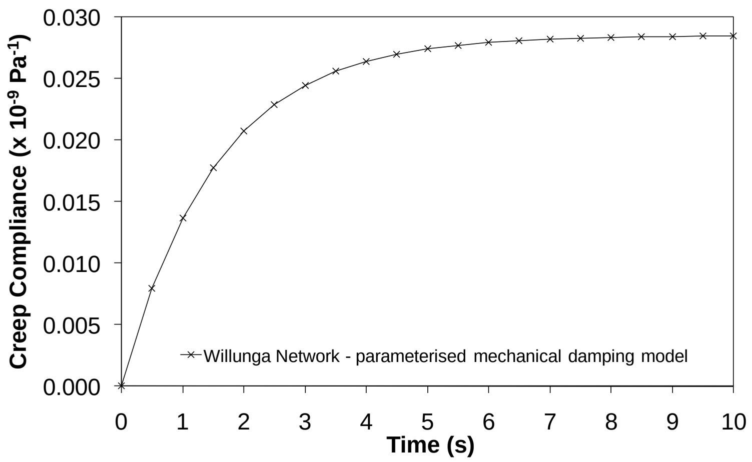

Figure 15 – Parameterized creep compliance function after calibration of the conceptual mechanical damping transient model to measured responses at stations 1, 2 and 3

The comparisons between the measured and calibrated transient responses of the Willunga Network at stations 1, 2 and 3 (i.e., all measurement stations for the tests conducted with the transient generator located at point A), for a typical controlled transient test over a time scale of 4s, are illustrated in Figures 16, 17 and 18. The comparisons over a time scale of 14s are illustrated in Figures 19, 20 and 21. The calibrated transient responses at all three measurements locations were obtained using the parameters derived for the model with a 20m pipe reach discretisation (i.e., J = 0.29e-10 Pa^{-1} and Tau = 1.528s).

When calibrated viscous damping is included, there is a significant reduction in the error variance values obtained, with an average value of 3.3 for the three model discretisations, relative to an average value of 58.1 obtained for the conceptual unsteady friction calibration model. An even more significant reduction occurs relative to the error variance obtained using the non-parameterized unsteady friction transient model presented above, with only the theoretical contribution of unsteady friction taken into account, of 261.0. Dispersion and damping is accurately predicted over the short term as shown in Figures 16, 17 and 18 and long term as shown in Figures 19, 20 and 21. Significantly, the action of the viscous mechanism is able to damp the predicted response as soon as the first pressure wavefront arrives (i.e., after the first change in pressure). This supports the hypothesis that mechanical damping, and not fluid friction, is dominant for the Willunga Network.

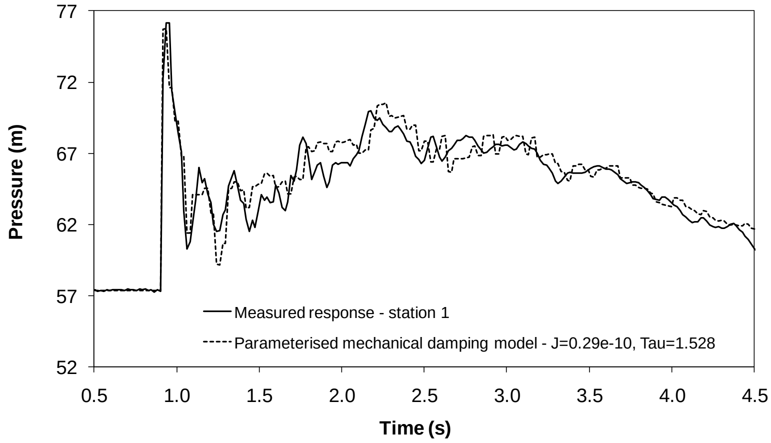

Figure 16 – Measured and predicted responses for station 1 in the Willunga Network using a conceptual (parameterized) mechanical damping model over a time period of 4s

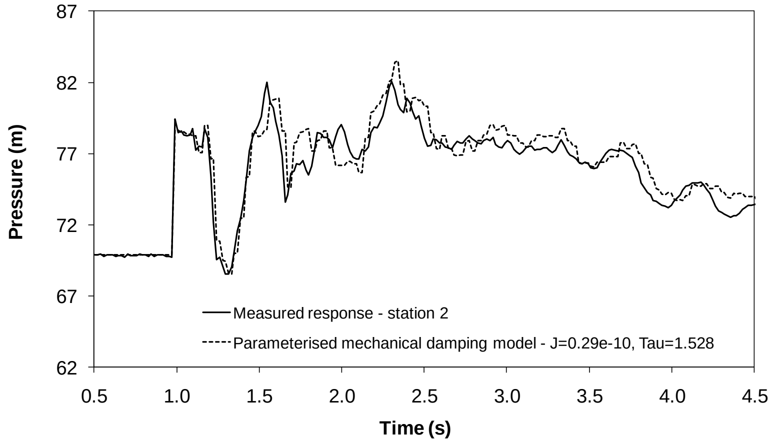

Figure 17 – Measured and predicted responses for station 2 in the Willunga Network using a conceptual (parameterized) mechanical damping model over a time period of 4s

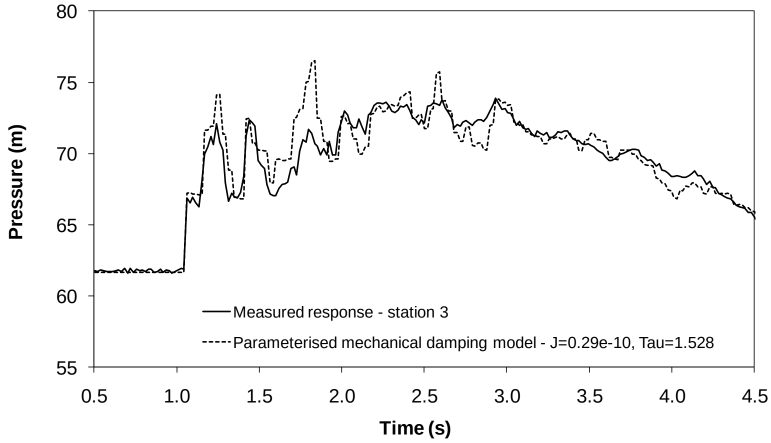

Figure 18 – Measured and predicted responses for station 3 in the Willunga Network using a conceptual (parameterized) mechanical damping model over a time period of 4s

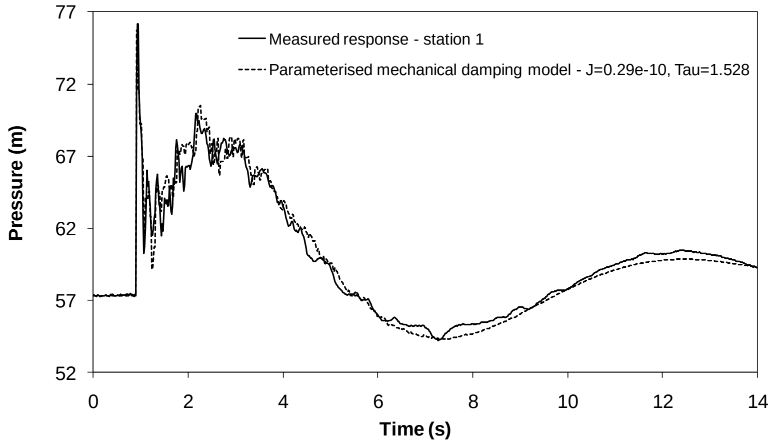

Figure 19 – Measured and predicted responses for station 1 in the Willunga Network using a conceptual (parameterized) mechanical damping model over a time period of 14s

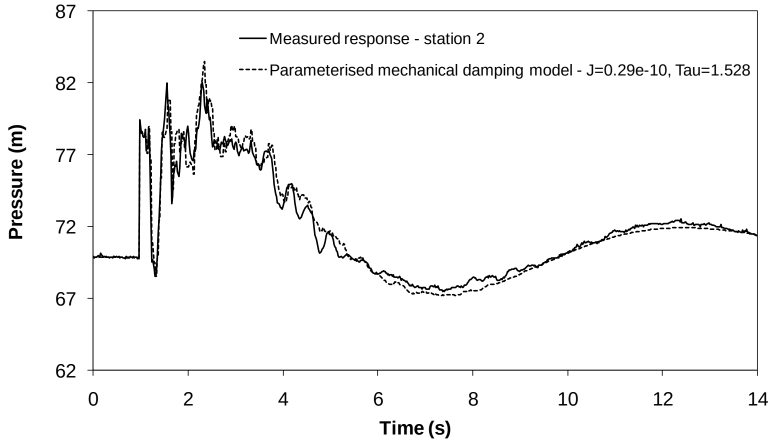

Figure 20 – Measured and predicted responses for station 2 in the Willunga Network using a conceptual (parameterized) mechanical damping model over a time period of 14s

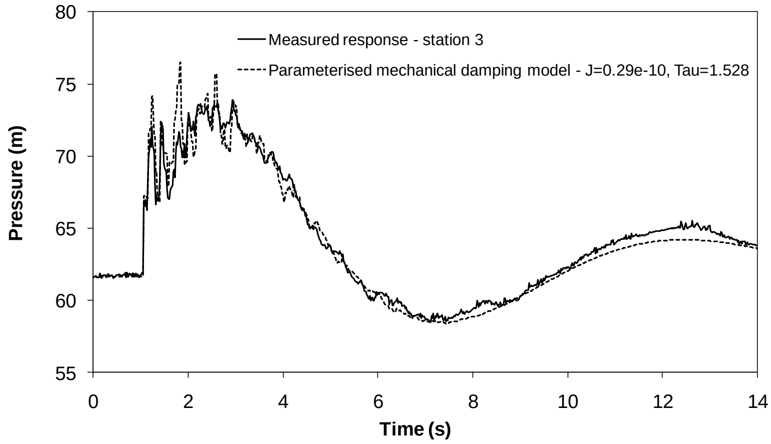

Figure 21 – Measured and predicted responses for station 3 in the Willunga Network using a conceptual (parameterized) mechanical damping model over a time period of 14s

The unsteady friction and mechanical damping conceptual models both utilise two parameters to globally compensate for dispersion and damping via the conceptual modification of a weighting function and creep compliance curve, respectively. Furthermore, the implementation of each mechanism in conceptual transient models, via efficient recursive approximations, is similar. The significant difference is that the unsteady friction weighting function acts to incorporate dispersion and damping via the momentum equation whereas the creep compliance curve acts via the continuity equation.

Validation

As described above, transient field tests were undertaken with the transient generator installed at two separate locations shown as points A and B in Figure 2. The results from the tests conducted with the transient generator located at point A have been used for the calibration of the unsteady friction and mechanical damping conceptual models. The results from the tests conducted with the transient generator located at point B will be used, with the calibrated parameters from the tests with the transient generator located at point A (obtained using the mechanical damping conceptual model), to validate the calibration. Validation will be demonstrated by using the parameters from the calibration tests to predict the transient response of the Willunga Network when the transient is generated at a different location (i.e., point B) without the requirement for any re-calibration.

As mentioned above, only stations 2 and 3 were deployed for the tests with the transient generator installed at point B. The comparison between the measured and predicted transient response of the Willunga Network at station 2, for a typical controlled transient test over a time scale of 4s with the transient generator located at point B, is illustrated in Figure 22. A similar comparison of the measured and predicted transient response at station 3 is illustrated in Figure 23. The comparison between the measured and predicted transient responses at stations 2 and 3 over a time scale of 14s is illustrated in Figures 24 and 25, respectively. A 10mm discharge nozzle was installed when the transient generator was located at point B. This is why the magnitude of the maximum transient pressures measured at stations 2 and 3 are less for the tests conducted with the transient generator located at point B rather than point A. The shape of the transient responses measured at stations 2 and 3 changes significantly with the change in location of the transient generator from point A to B for the two sets of tests.

The results show that dispersion and damping is accurately predicted over the short and long term using the previously calibrated parameter values for the mechanical damping conceptual model (i.e., J = 0.29e-10 Pa^{-1} and Tau = 1.528s). Confirmation that re-calibration is not required suggests that the mechanical damping is consistent across the Willunga Network and can be successfully predicted throughout the network based on a limited number of calibration tests (i.e., one test for the Willunga Network).

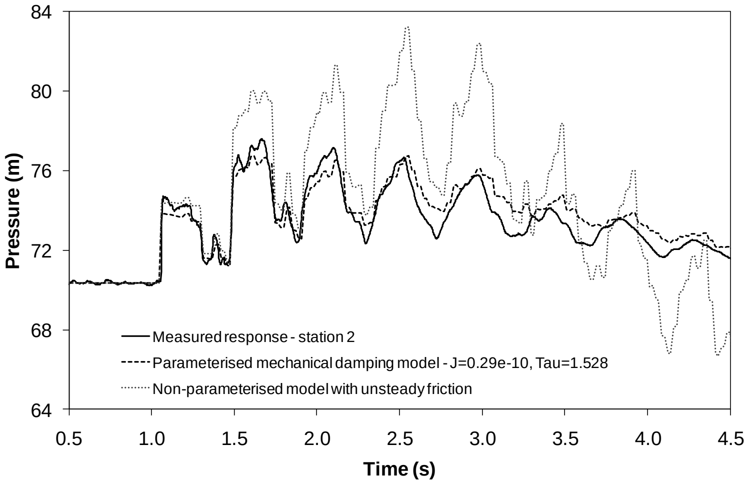

Figure 22 – Measured and predicted responses for station 2, with the Transient Generator at a new location, using a conceptual (parameterized) mechanical damping model, over a time period of 4s, and fixed pre-calibrated parameters from a previous calibration test

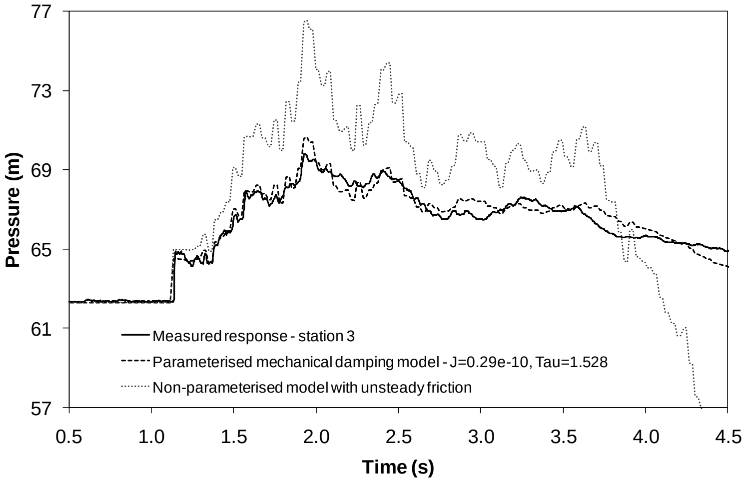

Figure 23 – Measured and predicted responses for station 3, with the Transient Generator at a new location, using a conceptual (parameterized) mechanical damping model, over a time period of 4s, and fixed pre-calibrated parameters from a previous calibration test

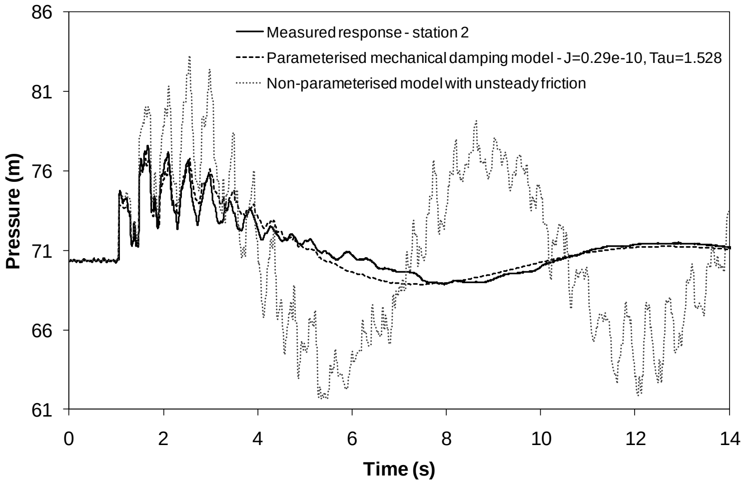

Figure 24 – Measured and predicted responses for station 2, with the Transient Generator at a new location, using a conceptual (parameterized) mechanical damping model, over a time period of 14s, and fixed pre-calibrated parameters from a previous calibration test

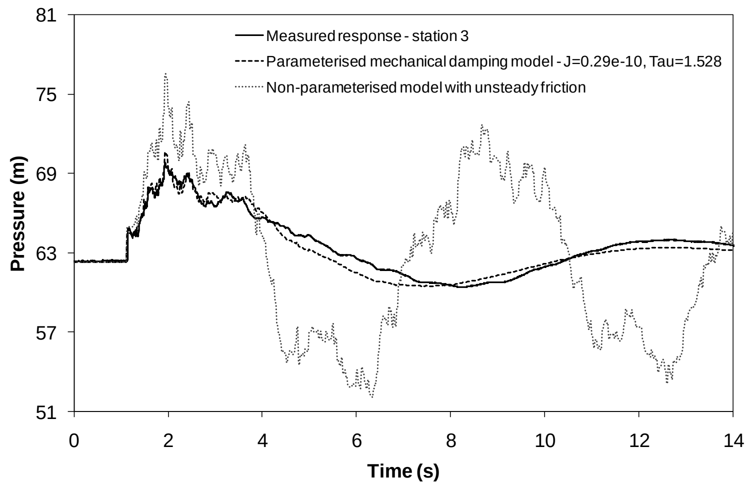

Figure 25 – Measured and predicted responses for station 3, with the Transient Generator at a new location, using a conceptual (parameterized) mechanical damping model, over a time period of 14s, and fixed pre-calibrated parameters from a previous calibration test

Summary and Conclusions

A review of the literature has shown that very limited field testing of transient models has occurred for water distribution networks and that there are significant discrepancies between measured responses and the responses predicted using traditional transient models. This paper reports the results of hydraulic transient testing on a water distribution network in the field and the development of a conceptual transient model able to replicate the measurements.

The reported field tests were conducted on a small town water distribution network comprising 4 km of pipe of homogenous material. Demand and leakage were able to be accurately measured. Furthermore, the network was able to be flushed prior to the field tests to assess and minimise the quantity of entrained air. Controlled transient events were induced using a custom built side discharge transient generator.

A quasi-steady friction transient model, which took into account the measured demand and leakage during the field tests, gave a poor match between measured and modelled response apart from the prediction of the initial pressure rise after the controlled transients were induced (error variance 265.7). An unsteady friction transient model was then used (without any parameterization for calibration) but only marginally improved the match between measured and modelled responses (error variance 261.0). Possible reasons for the discrepancies included effects from additional fluid friction losses from smaller lateral pipes and/or mechanical dispersion and damping caused by the interaction of the pipes and joints in the network with surrounding soils (including effects from variable pipe and joint restraint).

An unsteady friction based conceptual transient model was subsequently developed to account for the possible fluid friction losses associated with smaller lateral pipes (e.g., water service connections not directly included in the model). This conceptual model was based on a parameterisation of algorithms describing an unsteady friction weighting function. The model improved the match between measured and modelled responses (error variance 58.1). However, discrepancies between the magnitude of measured and predicted damping and dispersion, and between the phase of the measured and predicted transient responses, remained.

Finally, a mechanical damping based conceptual transient model was developed using an efficient algorithm for the calibration of spring and dashpot parameters comprising a Kelvin-Voigt mechanism. This mechanism was included to facilitate calibration for the effects of mechanical interaction and vibration of the pipes and joints in the network and the transmission of energy out of the fluid within the system into the surrounding media. This conceptual model significantly improved the match between measured and modelled responses (average error variance 3.3) suggesting the structure of the conceptual model was appropriate and that mechanical dispersion and damping was a significant influence on the waterhammer response of the network.

The measured responses for transient tests not used for calibration of the mechanical damping conceptual model were able to be accurately predicted using parameters calibrated for previous, and distinct, field tests. This validated the previously calibrated parameters and confirmed that the mechanical damping conceptual model only requires limited calibration before being used to more generally predict transient responses in a network of the scale of the Willunga Network.

Notation

A = cross-sectional area of pipe

a = wave speed

C = Hazen-Williams pipe conveyance factor

D = internal diameter of pipe

E_0 = elastic modulus of pipe wall

E_1 = modulus of elasticity of the creep deformation spring used in a single element Kelvin-Voigt model

g = gravitational acceleration

H = piezometric head

$H(x,t)$ = piezometric head at time t

$H_0(x)$ = steady state piezometric head

h = pipe wall thickness

h_{fU} = unsteady friction loss

J_0 = spring compliance associated with the elastic modulus

J_1 = spring compliance associated with the modulus of elasticity of the creep deformation spring

k = index for parameters m and n

m_k = multiplying parameter applied in recursive approximation of weighting function for calculating unsteady friction

m_{k+1} = multiplying parameter calibrated in conceptual unsteady friction model

N = number of parameters m and n used in approximate unsteady friction weighting function

n_k = exponential parameter applied in recursive approximation of weighting function for calculating unsteady friction

n_{k+1} = exponential parameter calibrated in conceptual unsteady friction model

Q = volumetric rate of flow

t = time

V = velocity of flow

W = unsteady friction weighting function

x = distance along pipe

$y_k(t)$ = recursive variable used in efficient calculation of unsteady friction

$y_m(t)$ = recursive variable used in efficient calculation of viscous damping

Δt = time step in transient model

Δx = pipe reach discretisation in transient model

α = pipe wall thickness factor

γ = specific gravity of water

ε_r = circumferential strain in pipe wall

ν = kinematic viscosity

μ_1 = viscosity of the dashpot used in a single element Kelvin-Voigt model

τ = dimensionless time

τ_1 = retardation time associated with the dashpot

$\Delta\tau$ = dimensionless time step = $4\nu\Delta t/D^2$

References

Budny D.D., Wiggert D.C. and Hatfield F.J. (1991) "Influence of structural damping on internal pressure during a transient pipe flow", *Journal of Fluids Engineering*, Transactions of the ASME, 113(3), pp 424-429

Covas D., Stoianov I., Mano J.F., Ramos H., Graham N. and Maksimovic C. (2004) "The dynamic effect of pipe-wall viscoelasticity in hydraulic transients: part I – experimental analysis and creep characterisation", Journal of Hydraulic Research, 42(5), pp 516-530

Gally M., Guney M. and Rieuford E. (1979) "Investigation of pressure transients in viscoelastic pipes", *Journal of Fluids Engineering*, Transactions of the ASME, volume 101, pp 495-499

Kagawa T., Lee I., Kitagawa A. and Takenaka T. (1983) "High speed and accurate computing method of frequency-dependent friction in laminar pipe flow for characteristics method", *Transactions of the Japanese Society of Mechanical Engineers*, volume 49 (447), pp 2638-2644 (in Japanese)

Karney B.W. and Fillion Y.R. (2003) "Energy dissipation mechanisms in water distribution systems", *Proceedings of the 4th ASME/JSME Joint Fluids Engineering Conference*, Volume 2, Part D, Symposia, pp 2771-2778

Kwon H.J. (2007) "Computer simulations of transient flow in a real city water distribution system", KSCE Journal of Civil Engineering, Korean Society of Civil Engineers, Volume 11, No.1, pp 43-49

McInnis D. and Karney B.W. (1995) "Transients in distribution networks: Field tests and demand models", *Journal of Hydraulic Engineering*, 121 (3), pp 218-231

Stephens M.L. (2008) "Transient Response Analysis for Fault Detection and Pipeline Wall Condition Assessment in Field Water Transmission and Distribution Pipelines and Networks", PhD Thesis, School of Civil, Environmental and Mining Engineering, the University of Adelaide, Adelaide, South Australia

Vardy A.E. and Brown J.M.B. (1995) "Transient, turbulent, smooth pipe friction", *Journal of Hydraulic Research*, 33(4), p 435

Vardy A.E. and Brown J.M.B. (2004a) "Transient turbulent friction in fully rough pipe flows", *Journal of Sound and Vibration*, 270(1-2), pp 233-257

Vitkovsky J.P., Stephens M., Lambert M.F., Simpson A.R. and Bergant A. (2004) "Efficient and accurate calculation of Zielke and Vardy-Brown unsteady friction in pipe transients", *9th International Conference on Pressure Surges*, BHR Group, Chester, England, UK

Williams D.J. (1977) "Waterhammer in non-rigid pipes: precursor waves and mechanical damping", *Journal of Mechanical Engineering Science*, 19(6), pp 237-242

Wylie E. B. (1984) "Simulation of Vaporous and Gaseous Cavitation", *Journal of Fluids Engineering*, 106, pp 307-311

Zielke W. (1968) “Frequency-dependent friction in transient pipe flow”, *Journal of Basic Engineering*, Transactions of the ASME, 90(1), pp 109-115